Journal of

NANOSTRUCTURES

JNS
NANOSTRUCTURES
JNS.kashanu.ac.ir

Synthesis, Characterization and Catalytic Activity of CuO Nanostructures using Schiff Base Copper Complexes as a Precursor

L. A. Saghatforoush[*a], S. Sanati[a], Gh. Marandi[b], M. Hasanzadeh[c]

[a]*Department of Chemistry, Payame Noor University, 19395-4697, Tehran, I.R. of Iran*
[b]*Shahid Bakeri High education Center of Miandoab,Urmia University,Urmia,Iran*
[c]*Drug Applied Research Center, Tabriz University of Medical Sciences, Tabriz, Iran.*

Corresponding author:
E-mail address*:*
saghatforoush@gmail.com
Phone: +98-461-2349868
Fax: +98-461-2332566

Abstract

Two Cu(II) complexes, $[Cu(L_1)_2](NO_3)_2$ (1) and $[Cu(L_2)_2]$ $(NO_3)_2$(2), which L_1 and L_2 Schiff base ligands are 2-(thiophene-2-yl) -1*H*-imidazo [4,5-*f*] [1,10] phenanthroline and 2-(furane-2-yl)-1*H*-imidazo[4,5-*f*] [1,10] phenenthroline, respectively, were synthesized and characterized by physico - chemical and spectroscopic methods. Corresponded CuO nanoparticles were prepared by calcination of the obtained complexes at 500˚C. The structure of nano sized copper oxides were characterized by X- ray diffraction (XRD) and scanning electron microscopy (SEM). Electrocatalytic oxidation of acetylcholine (ACh) on copper oxide nanostructures were investigated. The results showed that acetylcholine (ACh) was oxidized irreversibly on copper oxide nanostructures with an excellent catalytic activity.

1. Introduction

Metal complexes with Schiff base ligands have played an important role since the early days of coordination chemistry [1]. Indeed, a great deal of work has been carried out on the synthesis and characterization of transition metal complexes with these type ligands, mainly due to their applications in organic chemistry, as liquid crystals and in catalytic processes [2]. Due to their optoelectronic properties, aryl imidazo phenanthrolines play important roles in materials science and medicinal chemistry. Therefore, they have found application as ligand for the synthesis of metal complexes of ruthenium(II), copper(II), cobalt(II), nickel(II), manganese(II) and several lanthanides especially for nonlinear optical (NLO) applications[3-4]. Nanostructure metal oxides have been attended in the field of nanotechnology both from a fundamental and industrial point of view. For example, their peculiar electrical properties make

them suitable as active sensing materials in resistive sensors, with enhanced performance in comparison to bulk materials. Copper oxide is an important transition metal oxide with many practical applications, such as it is the basis of several high-Tc superconductors and materials with giant magnetoresistance [5-10], and is also used as catalysts, pigment, p-type semiconductor, gas sensors, solar cells, magnetic storage media and cathode materials [11,12]. Because of the practical reasons mentioned above, the synthesis of nanostructured CuO has also attracted considerable attention. The thermal decomposition of transition-metal complexes is one of the simplest and least expensive techniques for preparing nanosized transition-metal oxides [13-20]. This technique is simple and do not need for a template and complex apparatus. By selecting an appropriate precursor coupled with a rational calcinations procedure, products with nano sizes could be obtained. This method also has potential advantages, including high yield of pure products, absence of solvent, and exempting the need for special equipment.

In this paper, we describe the synthesis and characterization of two new copper(II) complexes of Schiff base ligands namely 2- (thiophene-2-yl) -1*H*-imidazo[4,5-*f*] [1,10] phenanthroline(L$_1$) and 2-(furane-2-yl)-1*H*-imidazo[4,5-*f*][1,10] phenanthroline (L$_2$). CuO nanoparticles were prepared via the decomposition of the corresponded copper Schiff base precursor complexes at 500 ˚C. Electrocatalytic oxidationof acetylcholine (ACh) on copper oxide nanostructures was investigated.

2. Experimental

2.1. Materials and Characterization

All reagents were purchased from Merck and Fluka and used without further purification.

Elemental analyses (C, H, N) of the ligand and the metal complexes were performed with a Vario EL(III), CHN analyzer. The molar conductance values of the complexes were measured in DMF at room temperature using a Metrohm conductometer. The electronic spectra of the complexes in methanolic solution were recorded on a Perkin-Elmer lambda 25 spectrophotometer. FT-IR spectra (KBr pellet, 400–4000 cm^{-1}) were recorded on a Shimadzu FTIR model Prestige 21 spectrometer. ^{1}H NMR spectra of the ligands were recorded with a Bruker DRX-400 Avance instrument using CDCl$_3$ as the applied solvent. X-ray powder diffraction (XRD) measurements were performed using a Philips diffractometer manufactured by X'pert with monochromatized CuKa radiation. The samples were characterized using a scanning electron microscope (SEM) (Philips model XL30) with gold coating.

Electrochemical measurements were carried out in a conventional three-electrode cell powered by an electrochemical system comprising an AUTOLAB system with PGSTAT302N boards (Eco Chemie, Utrecht, the Netherlands). The system was run on a PC using ANOVA software. A saturated calomel electrode (SCE) was a reference electrode. All potentials were measured with respect to the SCE which was positioned as close to the working electrode as possible by means of a luggin capillary.

2.2. Procedure for preparation of ligands (L$_1$, L$_2$)

L$_1$: A methanolic solution (15 ml) containing 1 mmol (0.21g) of 1,10-phenanthroline 5,6-dione was added to a solution of 2–thiophen carbaldehyde (0.112 g, 1 mmol), amoniume acetate (0.929 g, 1.2 mmol) and triethyl amine (0.03ml) in absolute methanol (15 ml). The

resulting solution was refluxed for 2h and then cooled to room temperature. The resulting's precipitates were washed with a small amount of cooled diethyl ether, dried and characterized as the pure compounds. Yield: 0.22 g (73%). Anal. Found: C, 67.9. H, 2.98.N, 18.1.Calcd: C, 67.5, H, 3.3, N, 18.5%. m.p: >320°C. FT-IR (KBr disk): 3421, 3070, 1600, 1570cm^{-1}. ^{1}H NMR (400 MHz CDCl$_3$) dH: 14.15 (S, 1H), 9.1 (dd, 2H), 9.02 (dd, 2H), 8.9(d,brs, 2H), 8.05(d, 1H), 7.76(d, 1H), 7.28(t, 1H). ^{13}C NMR (CDCl$_3$) δ_C: 123.06, 125.31, 125.77, 126.12, 126.74, 127.37, 127.52, 128.72, 129.47, 141.18, 129.86, 132.28, 142.51, 146.56, 148.44, 148.49, 151.47. (Fig1. A)

L$_2$: L$_2$ was synthesized in the same way as L$_1$ using 2–furane carbaldehyde instead of 2–thiophen carbaldehyde (0.096 g, 1 mmol).

Yield: 0.20 g (68%). Anal. Found: C, 71.7. H, 3.1.N, 19.9.Calcd: C, 71.3. H, 3.4.N, 19.5%. m.p: 195 °C. FT–IR (KBr disk): 3076, 1577, 3420cm^{-1}. ^{1}H NMR (400 MHz CDCl3) δH: 9.01 (dd, 2H), 8.90 (dd, 2H,), 7.79 (m, 2H), 7.9(d, 1H), 7.27(d, 1H), 6.7(dd, 1H). ^{13}C NMR (CDCl3) δ_C: 113.09, 116.75, 121.69, 121.84, 122.37, 122.61, 127.57, 129.06, 129.83, 142.24, 142.30, 142.77, 143.79, 144.22, 144.77, 146.84, 148.61. (Fig1. B).
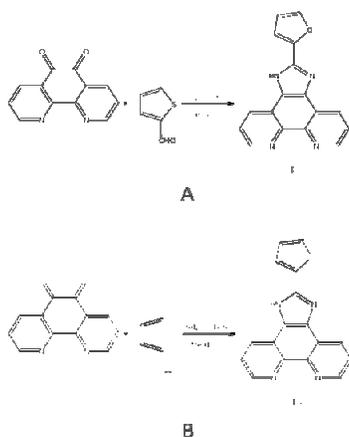
Fig. 1. (A, B). Schematic representation of syntheses of the Schiff base ligands (L$_1$, L$_2$).

2.3. Preparation of the copper complexes (1-2)

A solution of copper nitrate trihydrate (0.241g, 1mmol) in absolute methanol (10 ml) was added to a solution of ligand in absolute methanol (10 ml). The mixture was refluxed for 24h, the obtained yellow precipitates were washed well with cooled diethyl ether and dried.

[Cu(L$_1$)$_2$](NO$_3$)$_2$ (1), Yield: 0.24 g (58%). Anal. Found: C. 52.1, H. 2.8, N. 17.1, Calcd: C. 51.5, H. 2.5, N. 17.6%. m.p: 160 °C. IR (KBr disk): 3076, 1600, 1629, 1380cm^{-1}.

[Cu(L$_2$)$_2$] (NO$_3$)$_2$ (2), Yield: 0.215 g (53%). m.p: 95 °C. CHN. Found: C. 53.1, H. 2.69, N. 18.5. Calcd: C. 53.7, H. 2.63, N. 18.4%. IR (KBr disk): 3076, 1634, 1619,1384 cm^{-1}. (Fig. 2).
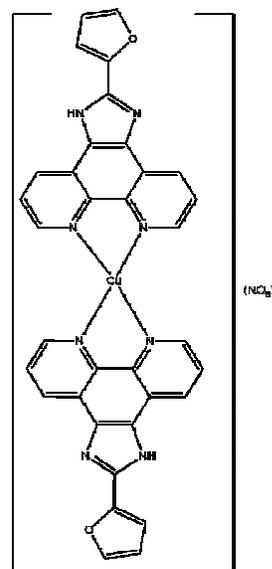
Fig. 2. Suggested structure of complex 2.

2.4. Preparation of the nano copper oxides

To prepare CuO nanoparticles, the complexes were added to a porcelain crucible and placed in an electric furnace. The each complex was heated to 200 °C in air for 2h. Similar experiments were performed with the complex at the selected temperatures of 300, 400, and 500 °C. The decomposition product generated from the complex

at each temperature was cooled to room temperature and collected for characterization. The most suitable product (pure CuO) was achieved in 500 ˚C.

2.5. Preparation of unmodified CPE and copper oxide electrodes

Unmodified carbon paste electrode (UCPE) was prepared by hand-mixing carbon powder and mineral oil (80/20 w/w %) ratio. The paste was carefully mixed and homogenized in an agate mortar for 20min. The resulting paste was kept at room temperature in a desiccator. The paste was packed firmly into a cavity (3.6mm diameter, geometric surface area of $0.1017cm^2$ and 0.5mm depth) at the end of a Teflon tube. Electrical contact was established via a copper wire connected to the paste in the inner hole of the tube. The electrode surface was gently smoothed by rubbing on a piece of weighing paper just prior to use. This procedure was also used to regenerate the surface of the carbon paste electrodes. The copper oxide nanostructure-modified carbon paste electrodes (CONM-CPE) were prepared by mixing carbon powder together with copper oxide or nanoparticles at different ratios in an agate mortar until a uniform paste was obtained. The percentage (w/w) of copper oxide informed throughout the text corresponds to the final percentage relative to the total paste composition. Then mineral oil was added (20 w/w %) and mixed thoroughly. The obtained paste was packed into a 3mm diameter cavity at the end of a Teflon tube, and the electrical contact was provided with a copper wire. The effect of the modifier percentage was examined on the intensity of acetylcholine oxidation peak current on the carbon paste electrode was examined. The highest peak current for the modified carbon paste electrode was obtained

when the content of the modifier was 20% in the paste of course, in concentrations more than 20%, a slight decrease in the current was observed which could be attributed to reduction of the electrode surface conductivity. With all these results taken in to account, carbon paste having 20% CuO nanoparticles, 60% graphite and 20% mineral oil was used for later studies.

3. Results and discussion

Both complexes are soluble in most of the common organic solvents. The infrared spectra of the free ligands and its complexes were recorded in the region 4000–400 cm^{-1}. The ν(C-H) aromatic rings, ν(C=C), ν(N-H) imidazol ring stretching vibrations of free ligands are observed at 3076, 1577 and 3420 cm^{-1}, respectively. The ν(C =N) stretching vibration of azomethine group in the free ligands (1600–1629 cm^{-1}) is shifted to lower frequency by 16–39 cm^{-1} in the complexes, indicating that the ligands are coordinated to metal ion through the nitrogen atom of the azomethine group [10]. The presence of uncoordinated nitrate as counter ion in both complexes are associated with absorptions at 1380-1384 cm^{-1} [11-12]. The ^{1}H NMR spectrum of the free schiff base ligands in chloroform displays seven signals for L_1 and six signals for L_2 assigned to the aromatic protons of L_1 and L_2. The ^{13}C NMR spectrum of L_1 and L_2 in chloroform displays 17 distinct signals assigned to the aromatic carbon atoms. The molar conductivity data at room temperature show that both complexes are 2:1 electrolytes.

The electronic spectral data in methanol solution suggest basically square planar geometry for both copper complexes. In general square-planar complexes are known to exhibit one or two bands. Complexes 1 and 2 show a broad band for the d–d transitions at 698 and 688 nm, respectively. The

appearance of similar d-d transitions in both 1 and 2 confirms the semi-coordinated character of the pyridinic nitrogen of the ligands in 1 and 2, which does not significantly affect the square planar geometry around the Cu(II) ions of the complexes. At the higher energy region, the ligand to metal charge transfer bands were located for both the complexes. The presence of band at 327nm in both complex can be assigned to $\Pi \rightarrow \Pi^*$ imidazol transitions (Fig 3(A, B)).

copper oxide (CuO), which are consistent with the standard reported values (JCPDS File no. 41-0254). The broadening peaks indicates that the articles were of nanometer scale. Particle size estimated from the Scherrer formula, D= 0.891/ β cosθ, where D is the average size, λ is the X-ray wavelength (0.154 nm), and θ and β are the diffraction angle and full- width at half maximum of an observed peak respectively. The average size of the CuO nanoparticles were calculated about 43nm by using the strongest peak (111) at 2θ = 38.8.

Fig. 3. (A): UV–Vis spectra of complex (1), (B): UV–Vis spectra of complex (2).

To prepare CuO nanoparticles, the complexes were calcinated at 500 ˚C in air for 2 h. Fig. 4 shows the SEM images of the CuO nanostructures obtained from calcination of complexes (1) and (2) under air.

Fig. 5 shows the X-ray diffraction (XRD) pattern of the CuO. All the peaks correspond to the reflections from (110), (002), (111), (202), (020), (202), (113), (311), (220) planes of monoclinic

Fig. 4. SEM images of copper(II) nano oxides from complex 1 (A),complex 2 (B).
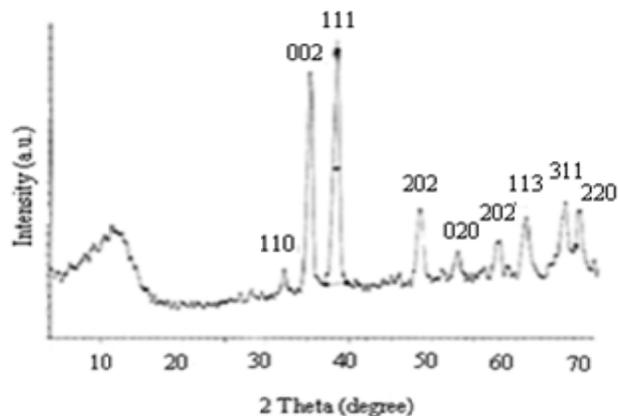
Fig. 5. XRD pattern of CuO nanostructures

Fig. 6 shows the optical absorption spectra of CuO nanoparticles, dispersed in methanol. The copper nanoparticles prepared display an absorption peak at around 280 nm and a shoulder at about 296 nm. These peaks can be assigned to the absorption of nanoparticles of copper oxides [21]. The presence of these two peaks and the broadness of the absorption peaks probably stems from the wide size distribution.
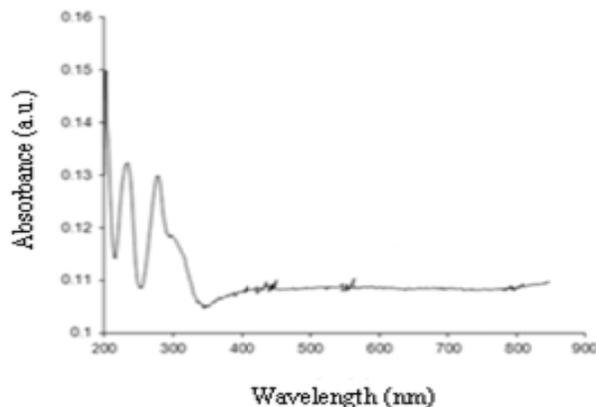
Fig. 6. The optical absorption spectra of CuO nanoparticles

3.1. Electrochemical study

ACh is the earliest discovered neurotransmitter which has an important function in the cholinergic system where it acts as a transmitter of impulses on the cholinergic synapses[22]. It can be found in the central nervous system, neuromuscular junctions, spinal cord, and preganglionic and motor neurons. Unfortunately, Achis neither easily oxidizable/ reducible norpossesses structural characteristics (electroreactive, chromophore or fluorophore groups) allowing a sensitive detection using electrochemical, spectrophotometric or fluorometric methods. Therefore, well established methods typically used for other neuro transmitters are useless and the majority of the methods developed for its determination generally require a conversion into more easily detectable compounds[23].

In this work CuO nanostructures have been used for electrocatalytic oxidation and determination of ACh in aqueous solution. The electrocatalytic activity of CONM–CPE was examined by cyclic voltammetry. Fig. 7Ashows that there are no CV peaks for the bare CPE electrode in the presence and absence of ACh;the figure shows that there is a remarkable increase in the anodic peak current density for the modified electrode after the addition of Ach (Fig. 7 B), with reference to the anodic peak current density of the modified electrode before its addition. This increase is indicative of the excellent electrocatalytic activity of the CuO nanostructures toward ACh. Fig. 7 C clearly shows that the CPE electrode itself has no response for ACh and only after its modification with CuO nanostructures it shows its response to ACh; this indicates the catalytic ability of the modified electrode.
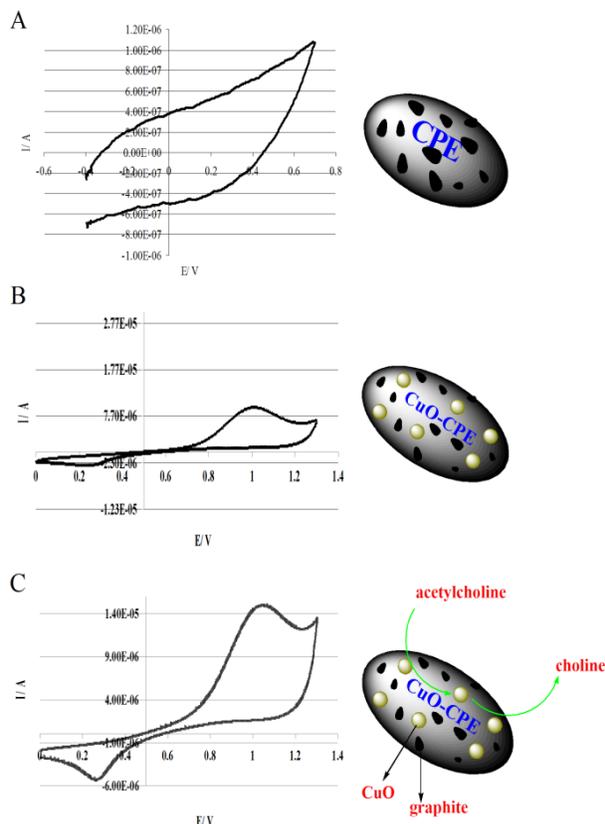
Fig. 7. Cyclic voltammograms of CPE (**A**) and CONM-CPE in 0.1 M NaOH at scan rate 50 mV s^{-1} in the absence (**B**) and presence 1mM ACh (**C**).

Fig. 8A shows the CV responses of CONM-CPE in 0.1 M NaOH solution containing various concentrations of ACh, *i.e.,* 1.0, 2.0, and 3.0 mM. The apparent and linear increase in oxidation peak current at the potential of about 0.997 V indicates that the modified electrode can be applied for the detection of ACh with high sensitivity. In addition, the mechanism of the electrocatalysis can be shown by the following equations:

$$Cu(I) + OH^- \rightarrow Cu(II) - (OH^-) + e^- \quad (1)$$

$$Cu(II) - (OH^-) + ACh \rightarrow Cu(I) + OH^- + Choline \quad (2)$$
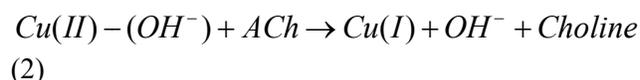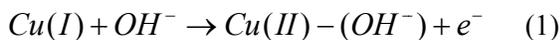
It should be noted here that the anodic peak potential shifts slightly to more positive values with increasing concentration of ACh, which can be attributed to the change in pH value due to the

production of Choline. To further confirm this point, we have also obtained the CV responses of CONM–CPE in 1.0 M NaOH solution containing various concentrations of ACh, *i.e.,* 1.0, 2.0, and 3.0 mM.Fig.8B shows the CVs obtained in 1.0 M NaOH with different concentrations of ACh. It can be seen in Fig. 8A that the anodic peak potential shifts from 1.01 V to 1.03 V in 0.1 M NaOH, when the concentration of ACh increases from 0 to 3.0 µM. However, in Fig. 8B, the anodic peak potential shifts from 1.008 V to 1.08 V in 1.0 M NaOH, when the concentration of ACh increases from 0 to 3.0 µM. Thus the shift in the anodic peak potential becomes smaller, if 1.0 M NaOH is used. For the same amount of ACh, the potential shift is smaller in the case of 1.0 M NaOH than that in the case of 0.1 M NaOH, because the buffer capacity of 1.0 M NaOH is higher than that of 0.1 M NaOH. The change in pH value is smaller for the same amount of generated Choline in the case of 1.0 M NaOH. This result is in agreement with the above observation that the slight shift in the anodic peak potential with increasing concentration of ACh is to be attributed to the change in the pH value due to the production of choline.

In order to develop a biosensing procedure for sensing and determination of ACh, the amperometry technique was employed. Typical amperometric signals obtained during successive increments of ACh to the solution using CONM–CPE, where a working potential of 670mV was applied, are depicted in Fig. 9. The nanocomposite responses were proportional to the ACh concentration and CONM–CPE represented the highest sensitivity. The limits of detection (LOD) and quantitation (LOQ) of the procedure were calculated according to the 3S$_d$/m and 10 S$_d$ /m criteria, respectively, where S_d is the standard

deviation of the intercept and *m* is the slope of the calibration curves.

A

B
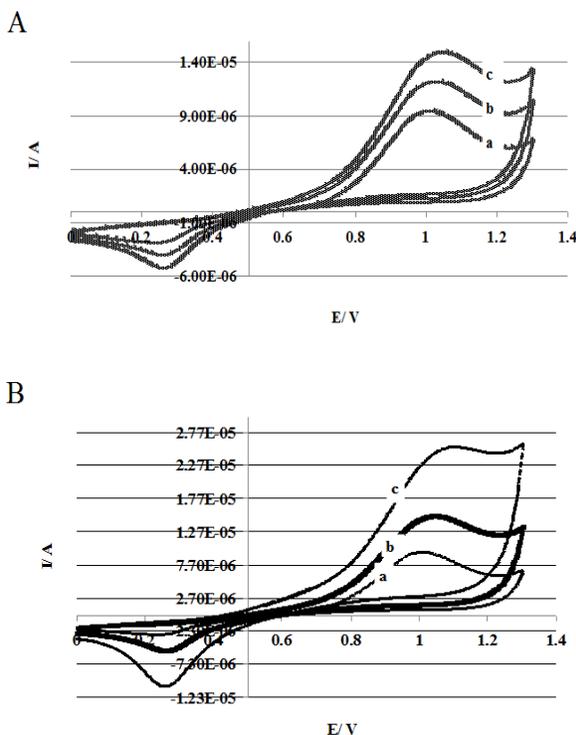
Fig. 8. Cyclic voltammograms of CONM-CPE in 0.1M (**A**) and 1.0 NaOH (**B**) buffer containing different concentration of ACh, 1.0, 2.0, and 3.0 mM.

   The determined parameters for calibration curves of ACh using CONM–CPE were obtained as LOD= 0.013 μM, LOQ= 0.02 μM, RSD = 3.11%, and a linear range of 0.01–1 μM. from the above results its find that, the present biosensor can determine ACh with a high sensitivity and a low limit of detection.
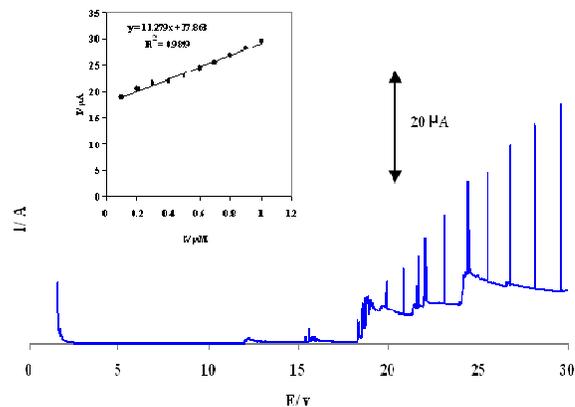
Fig. 9. Amperometric response at CONM-CPE held at 0.997 V in 0.1M NaOH for the successive addition of ACh. Inset: plot of chronoamperometric response *vs.* ACh concentration.

4. Conclusion

The present study describes the synthesis of two Cu(II) Schiff base complexes containing 2–(thiophene–2–yl)–1*H*–imidazo [4,5-*f*] [1,10] phenenthroline (L$_1$) and 2–(furane–2–yl)–1*H*–imidazo [4,5-*f*] [1,10] phenanthroline. Calcination of synthesized complexes were achieved corresponded CuO nanoparticles. We have presented electrochemical application of CuO nanoparticles. The electrooxidation of acetylcholine was successfully performed using the CuO nanostructures modified carbon paste electrode. The performance of the CuO nanosensor indicates that it can be used as a sensitive amperometric detector for sub-micromolar detection of acetylcholine.

Refrences

[1] L. Sacconi, Coord. Chem. Rev 1(1966) 126-132.
[2] L. Canali, D. C. Sherrintong, Chem. Soc. Rev 28 (1999) 85-93.

[3] H. Chao, Y.-X. Yuan, L.-N. Ji, Transition Met. Chem 29 (2004) 774-779.

[4] Y. Wei, Y. Yu, K. Wu, Cryst. Growth Des 7 (2007) 2262-2264.

[5] X.G. Zheng, C. N. Xu, Y. Tomokiyo, E. Tanaka, H. Yamada, Y. Soejima, Phys. Rev. Lett 85 (2000) 5170-5173.

[6] A. B. Kuz'menko, D. van der Marel, P. J. M. Van Bentum, E.A. Tishchenko, C. Presura, A. Bush, Phys. Rev. B 63(2001) 094303-094318.

[7] J. Tamaki, K. Shimanoc, Y. Yamada, Y. Yamamoto, N. Miura, N. Yamazoe, Actuators B 49 (1998)121-125.

[8] J. Chen, S.Z. Deng, N. S. Xu, W. X. Zhang, X.G. Wen, S. H. Yang, Appl. Phys. Lett 83 (2003) 746-749.

[9] M. Hossain, S. K. Chattopadhyay, S. Ghosh, Polyhedron 16 (1997) 1793-1802.

[10] S. Chandra, L. K. Gupta, Spectrochim. Acta A 60 (2004) 3079-3085.

[11] M. Shakir, S. P. Varkey, P. S. Hameed, Polyhedron 12(1993) 2775-2780.

[12] F. A. Cotton, J. J. Wise, Inorg. Chem 5 (1967) 1200-1207.

[13] S. Farhadi, J. Safabakhsh, J. Alloys Compd 515 (2012) 180 – 185.

[14] M. Salavati - Niasari, F. Davar, M. Mazaheri, Mater. Lett 62 (2008) 1890 –1892.

[15] M. Salavati - Niasari, F. Davar, Mater. Lett 63 (2009) 441– 443.

[16] M. Salavati - Niasari, F. Davar, M. Mazaheri, J. Alloys Compd 470 (2009) 502–506.

[17] F. Davar, Z. Fereshteh, M. Salavati - Niasari, J. Alloys Compd 476 (2009) 797–801.

[18] M. Salavati - Niasari, Z. Fereshteh, F. Davar, Polyhedron 28 (2009) 1065–1068.

[19] M. Khansari, A. Salavati - Niasari, F. Davar, Inorg. Chim. Acta 362 (2009) 4937–4942.

[20] M. Salavati - Niasari, N. Mir, F.Davar, J. Phys. Chem. Solids 70 (2009) 847–852.

[21] H. Wang, J-Z. Xu, J-J. Zhu, H-Y. Chen, J. Cryst. Growth 244 (2002) 88–94.

[22] S.M. Sine, Physiol. Rev 92 (2012) 1189-234.

[23] S. M. A. Shibli, K. S. Beenakumari, Electroanalysis 18 (2006) 465- 470.